Inorganic Chemistry

Article

pubs.acs.org/IC

Highly Porous 4,8-Connected Metal–Organic Frameworks: Synthesis, Characterization, and Hydrogen Uptake

David J. Mihalcik,† Teng Zhang,† Liqing Ma, and Wenbin Lin*

Department of Chemistry, CB#3290, University of North Carolina, Chapel Hill, North Carolina 27599, United States

Supporting Information

ABSTRACT: A series of highly porous 4,8-connected isoreticular MOFs of the **scu** topology $[Cu_4(\mathbf{L}_1)(H_2O)_4]\cdot 20DEF$, $[Cu_4(\mathbf{L}_2)(H_2O)_4]\cdot 16DMF\cdot 5H_2O$, and $[Cu_4(\mathbf{L}_3)(H_2O)_4]\cdot 14DMF$ ($\mathbf{L}_1$–$\mathbf{L}_3$ are (*R*)-1,1′-binaphthyl-derived octacarboxylate bridging ligands) were synthesized and characterized by single-crystal X-ray crystallography. Although the frameworks exhibit some distortion during the solvent removal process, the high-connectivity nature of the building blocks helps in stabilizing the frameworks, leading to high surface areas (S_{BET} = 1189–2448 m^2/g) and significant hydrogen uptake of up to 1.8 wt % (77 K, 1 atm).

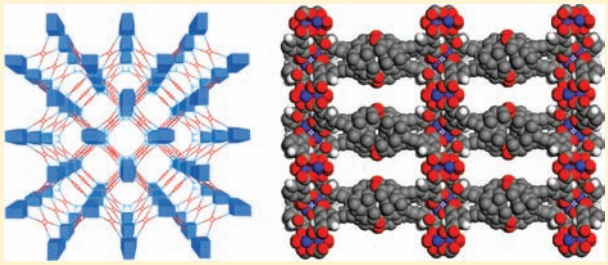

INTRODUCTION

Hydrogen is identified as one of the most promising alternative energy sources since no greenhouse gases or other environmentally detrimental molecules are emitted during energy extraction from hydrogen.[1,2] Storage and transportation of hydrogen however present a major challenge because of its very low boiling point. Several methods are being studied to facilitate hydrogen storage to meet transportation requirements. Conventional methods, such as liquefaction or compression of hydrogen gas, require cryogenic temperatures and/or extremely high pressures.[1,3] Chemisorption in alloys and metal hydrides, another storage method that has received significant consideration, suffers from binding hydrogen too tightly and is limited by slow charging/discharging rates, high releasing temperature, and poor reversibility.[2−5] Physisorption of hydrogen in porous materials provides an alternative strategy for hydrogen storage.[2,3,6]

As a class of new organic–inorganic hybrid materials, metal–organic frameworks (MOFs) have attracted increasing interest from chemists and materials scientists in the past decade.[7−11] Unlike traditional inorganic materials, MOF synthesis can be accomplished by combining organic synthetic methodologies and crystal engineering, allowing tuning of their properties for a variety of applications, including gas storage,[12−14] separations,[15−17] chemical sensing,[18−21] catalysis,[22−24] biomedical imaging,[25−27] and drug delivery.[28−30] MOFs present a particularly intriguing possibility for hydrogen storage as a result of their enormously porous structures with well-defined, uniform, and tunable pore sizes.[31−43] Interactions between hydrogen and the MOF framework can be enhanced by introducing open coordination sites at metal centers and aromatic ligands.[44] Further improvements in both hydrogen uptake capacity and hydrogen binding energy are however needed before MOFs can be considered for practical applications in hydrogen storage.

The choice of secondary building units (SBUs) is critical to successful synthesis of porous MOFs. Among several well-established SBUs,[45−49] the carboxylate-bridged copper paddle wheel $[Cu_2(O_2CR)_4]$ SBU is widely employed for constructing porous MOFs.[49−56] For example, the HKUST-1, which is built from copper paddle wheels and 1,3,5-benzenetricarboxylic acid, still serves as a benchmark material in both stability and gas uptake capacity.[49,57] Removal of the axially coordinated water molecules from the copper centers introduces open metal sites that enhance hydrogen–framework interaction and the gas uptake capacity.[44] However, the low connectivity (4) and planar nature of the copper paddle-wheel SBU makes it difficult to consistently synthesize isoreticular MOFs of the desired topology. For example, when linear dicarboxylate bridging ligands are used in combination with $Cu_2(O_2CR)_4$ SBUs, 2-D networks are expected based on topological considerations.[50,58]

It is now established that multicarboxylate bridging ligands are needed to build 3-D MOFs based on copper paddle-wheel SBUs.[37,59−67] Tetrahedral multicarboxylate linkers have been used to constructing such 3-D networks;[59−62,68] however, these 4,4-connected MOFs with large open pore and channel sizes tend to undergo severe framework distortion upon solvent removal, which lowers the porosity and gas uptake capacity.[59,60] We recently demonstrated the ability to construct 4,8-connect MOFs of the **scu** topology based on copper paddle-wheel and octacarboxylate ligands.[69] These 4,8-connected MOFs built from aromatic-rich bridging ligands show permanent porosity and robust structures for gas uptake applications.[69] In this work, we are extending this strategy to synthesize a series of 4,8-connected MOFs using chiral 1,1′-binaphthyl-derived aromatic-rich octacarboxylate ligands ($\mathbf{L}_1$–$\mathbf{L}_3$, Scheme 1). Large, permanent pore volumes and considerable surface areas are

Received: November 12, 2011
Published: January 6, 2012

   dx.doi.org/10.1021/ic2024296 | *Inorg. Chem.* 2012, 51, 2503–2508

Scheme 1. Synthesis of Octacarboxylic Acids L_1-H_8, L_2-H_8, and L_3-H_8

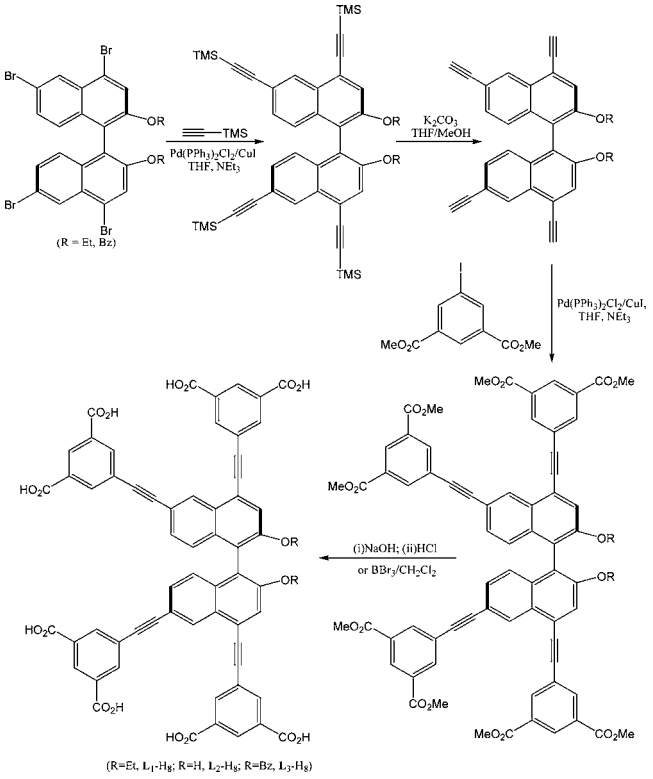

observed for these new MOFs, showing promise for potential applications in gas storage.

EXPERIMENTAL SECTION

$[Cu_4(L_1)(H_2O)_4]$·20DEF (1). A mixture of L_1-H_8 (1 mg, 0.91 μmol) and $Cu(ClO_4)_2$·$6H_2O$ (1.35 mg, 3.65 μmol) was dissolved in a solvent mixture of DEF (0.3 mL), H_2O (0.025 mL), and 1 M HCl (10 μL) in a screw-capped vial. The resulting solution was placed in an oven at 80 °C for 2 days. Blue-green crystals (2.2 mg, 69%) with a very thin plate shape were obtained after filtration. Solvent content calculated from the proposed formula: DEF, 58.8%; H_2O, 2.0%. Solvent content determined by ^{1}H NMR/TGA: DEF, 58.7%; H_2O, 1.9%.

$[Cu_4(L_2)(H_2O)_4]$·16DMF·$5H_2O$ (2). A mixture of L_2-H_8 (1 mg, 0.96 μmol) and $Cu(ClO_4)_2$·$6H_2O$ (1.42 mg, 3.85 μmol) was dissolved in a solvent mixture of DMF (0.1 mL), H_2O (0.050 mL), and 1 M HCl (10 μL) in a screw-capped vial. The resulting solution was placed in an oven at 80 °C for 4 h. Dark green crystals (1.8 mg, 75%) with a very thin plate shape were obtained after filtration. Solvent content calculated from the proposed formula: DMF, 44.6%; H_2O, 6.1%. Solvent content determined by ^{1}H NMR/TGA: DMF, 44.1%; H_2O, 6.3%.

$[Cu_4(L_3)(H_2O)_4]$·14DMF (3). A mixture of L_3-H_8 (1 mg, 0.82 μmol) and $Cu(ClO_4)_2$·$6H_2O$ (1.21 mg, 3.26 μmol) was dissolved in a solvent mixture of DMF (0.1 mL), H_2O (0.025 mL), and 2 M HCl (10 μL) in a screw-capped vial. The resulting solution was placed in an oven at 80 °C for 18 h. Green crystals (1.42 mg, 68%) with a very thin plate shape were obtained after filtration. Solvent content calculated from the proposed formula: DMF, 40.0%; H_2O, 2.8%. Solvent content determined by ^{1}H NMR/TGA: DMF, 40.5%; H_2O, 2.7%.

RESULTS AND DISCUSSION

1. Synthesis and Characterization of Ligands. The new 1,1′-binaphthyl-derived ligand, (*R*)-5,5′,5″,5‴-(2,2′-diethoxy-1,1′-binaphthyl-4,4′,6,6′-tetrayl)tetrakis(ethyne-2,1-diyl) tetraisophthalic acid (L_1-H_8), was synthesized by starting from a Pd-catalyzed Sonogashira coupling between 4,4′,6,6′-tetrabromo-2,2′-diethoxy-1,1′-binaphthyl and trimethylsilylacetylene followed by base-catalyzed deprotection (Scheme 1). The deprotected 4,4′6,6′-tetraacetylene intermediate was then treated with dimethyl 5-bromoisophtalate under Sonogashira coupling conditions. The resulting methyl ester was then either directly hydrolyzed to give the 2,2′-ethoxy-protected octa-acid compound (L_1-H_8) or subjected to a series of deprotection and hydrolysis steps to give the corresponding 2,2′-hydroxy ligand (L_2-H_8). 2,2′-Dibenzyloxy protected ligand L_3-H_8 was prepared in a similar manner, starting with the 2,2′-benzyl-protected tetrabromo compound in place of the 2,2′-ethoxy-protected intermediate.

2. Synthesis and Characterization of 4,8-Connected MOFs. Single crystals of $[Cu_4(L_1)(H_2O)_4]$·20DEF (**1**), $[Cu_4(L_2)(H_2O)_4]$·16DMF·H_2O (**2**), and $[Cu_4(L_3)(H_2O)_4]$·14DMF (**3**) were obtained by treating the corresponding ligands with $Cu(ClO_4)_2$·$6H_2O$ in DEF (diethylformamide) or DMF (dimethylformamide) at 80 °C (Scheme 2).

Scheme 2. Synthesis of MOFs 1−3

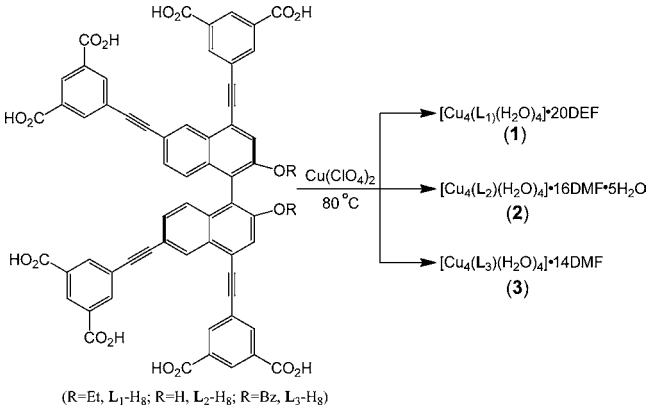

The formulas for **1**−**3** were established by a combination of thermogravimetric analysis (TGA), ^{1}H NMR spectroscopy, and single-crystal X-ray structure determination. To ensure consistent results, each sample was treated in exactly the same way for both TGA and ^{1}H NMR experiments. Fresh crystals were harvested by quick filtration and briefly dried on a piece of filter paper under air. The sample was then divided and loaded into a screw-capped vial with CD_3OD or the sample tray in TGA. The organic solvent inside the crystals is either DEF or DMF which has been exchanged by CD_3OD, and its exact amount was determined by calibrating against the internal standard, mesitylene. The total amounts of the solvents were obtained by TGA (Figure 1), and the amount of water molecules was calculated by subtracting DEF/DMF from the total solvent amount. The framework structures of **1**−**3** were unambiguously determined by single-crystal X-ray diffraction studies.

MOF **1** crystallizes in the tetragonal *P*4 space group. The asymmetric unit for the framework contains two copper atoms, one-half L_1 ligand, and two water molecules. The Cu atoms coordinate to four carboxylate oxygen atoms from four different L_1 ligands in the equatorial positions as well as a water molecule in the axial position, forming $[Cu_2(O_2CR)_4]$ paddle wheels as a 4-connected node. Each L_1 ligand is linked to eight different copper paddle wheels via the carboxylate groups, serving as an

dx.doi.org/10.1021/ic2024296 | Inorg. Chem. 2012, 51, 2503−2508

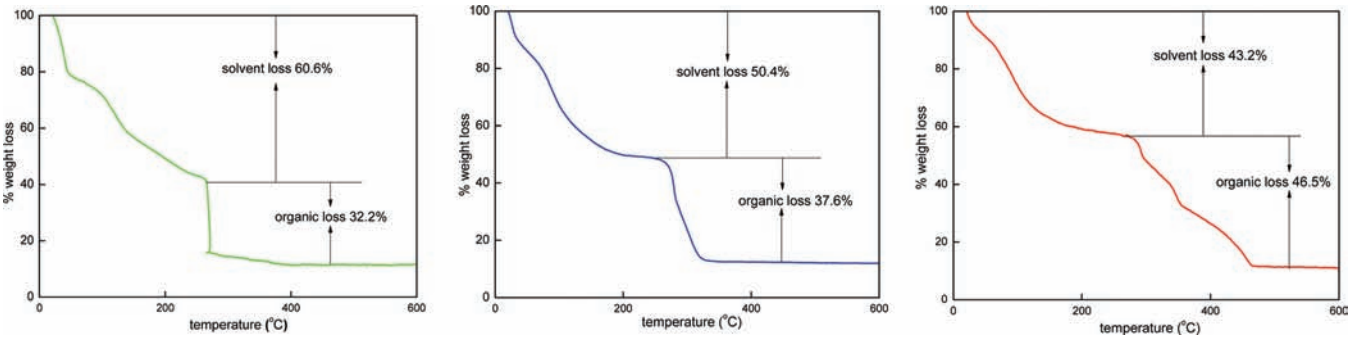

Figure 1. Thermogravimetric analysis (TGA) measurements for **1** (green), **2** (blue), and **3** (red).

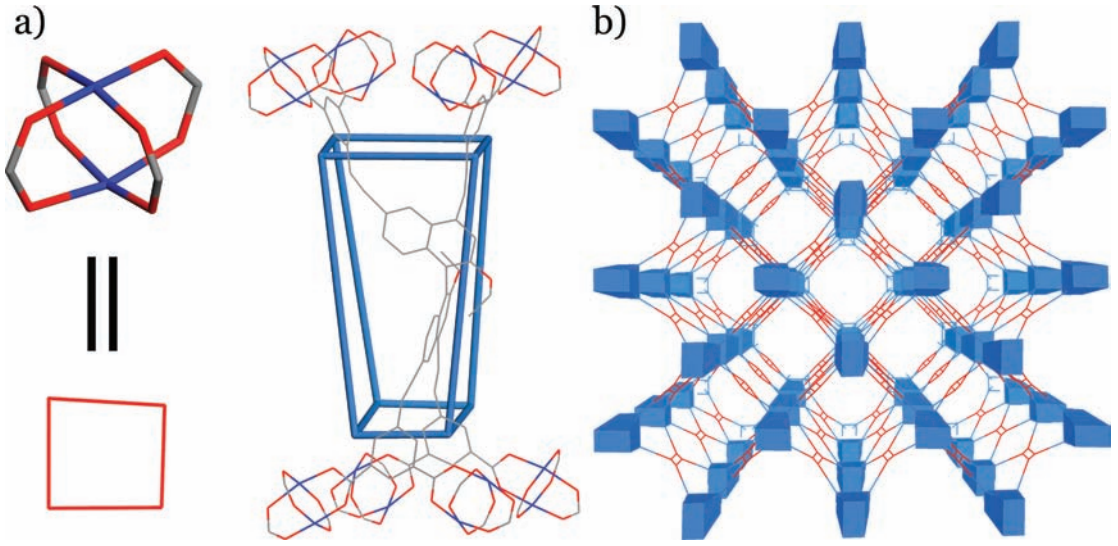

Figure 2. (a) $[Cu_2(O_2CR)_4]$ paddle wheels (represented as red rectangles) and their connectivity through the $\mathbf{L_1}$ ligand (represented as a blue prism). (b) Simplified connectivity scheme of **1** showing the **scu** topology.

8-connected node. As a result, **1** adopts the **scu** topology with the Schläfli symbol $\{4^4{\cdot}6^2\}_2\{4^{16}{\cdot}6^{12}\}$ (Figure 2).

MOF **3** is isostructural to MOF **1** with the same space group and connectivity, while MOF **2** crystallizes in the orthorhombic *C*222 space group and has very similar structural characteristics to MOFs **1** and **3**. The crystal structures of **1**−**3** are very similar to the MOFs built from the related 1,1′-binaphthyl-derived octacarboxylic acid,[69] indicating the robustness of the 4,8 connectivity in affording isoreticular MOFs.[70] Because of the elongated $\mathbf{L_1}$−$\mathbf{L_3}$ ligands, MOFs **1**, **2**, and **3** possess very large solvent-accessible volumes, constituting 67.9%, 70.3%, and 62.6% of the unit cell volume as calculated by PLATON,[71] respectively. Consistent with this, **1**, **2**, and **3** exhibited significant TGA solvent weight losses of 61%, 50%, and 41% in the 25−280 °C temperature range, respectively.

As shown in Figure 3c and 3d, MOF **2** possesses channels of ∼7 × 10.3 Å along the *c* axis and rectangular channels of ∼9.2 × 16 Å along the *b* axis. The ethoxy groups of the $\mathbf{L_1}$ ligands protrude into the open channels that run along the *c* axis and the (110) direction in **1**, thus reducing the open square channel sizes to ∼9.5 × 9.5 Å along the *c* axis and rectangular channels of ∼9.2 × 16 Å along the (110) direction. As expected, the bulkier benzyloxy groups in **3** reduce the open channel sizes even further, with the open channel of ∼7.2 × 7.2 Å along the *c* axis (Figure 3e) and the open channels of ∼6.0 × 6.7 and 6.7 × 7.8 Å along the (110) direction due to the protruding benzyloxy groups (Figure 3f).

MOFs **1**−**3** exhibit very high surface areas. The permanent porosity was established by nitrogen adsorption at 77 K (Figure 4) after a freeze-drying procedure.[72] Our previous work showed that severe framework distortion caused by the surface tension of the liquid phase can be minimized by freeze drying, leading to much enhanced porosities and surface areas as compared to conventional vacuum drying of the same samples.[61,72] The experimental Langmuir surface areas obtained for **1**, **2**, and **3** were 2245, 2819, and 1323 m^2/g, respectively (Table 1).[73] This porosity trend is consistent with the decreasing steric bulk of benzyloxy, ethoxy, and hydroxy groups on the 2,2′-position at the binaphthyl rings of the bridging ligands in **1**−**3**. However, the surface areas do not necessarily agree with the simulated N_2 adsorption isotherms calculated by the grand canonical Monte Carlo (GCMC) method,[74,75] which gave calculated Langmuir surface areas of 3947, 4027, and 3450 m^2/g for **1**, **2**, and **3**, respectively. This discrepancy suggests that the present MOFs have undergone some framework distortion when the included solvent molecules were removed during the freeze-drying processes. Upon desolvation, the elongated, partially flexible ligand can distort to lower the void space in the crystal and enhance stability. The experimental surface area of compound **3** was even much lower, which could be attributed to the partially flexible nature of the benzyloxy groups. Upon desolvation, a portion of pores can become adsorbate inaccessible as a result of the disordered orientations of benzyloxy groups. Because the GCMC simulations assume rigid ligand conformations, the

dx.doi.org/10.1021/ic2024296 | *Inorg. Chem.* 2012, 51, 2503−2508

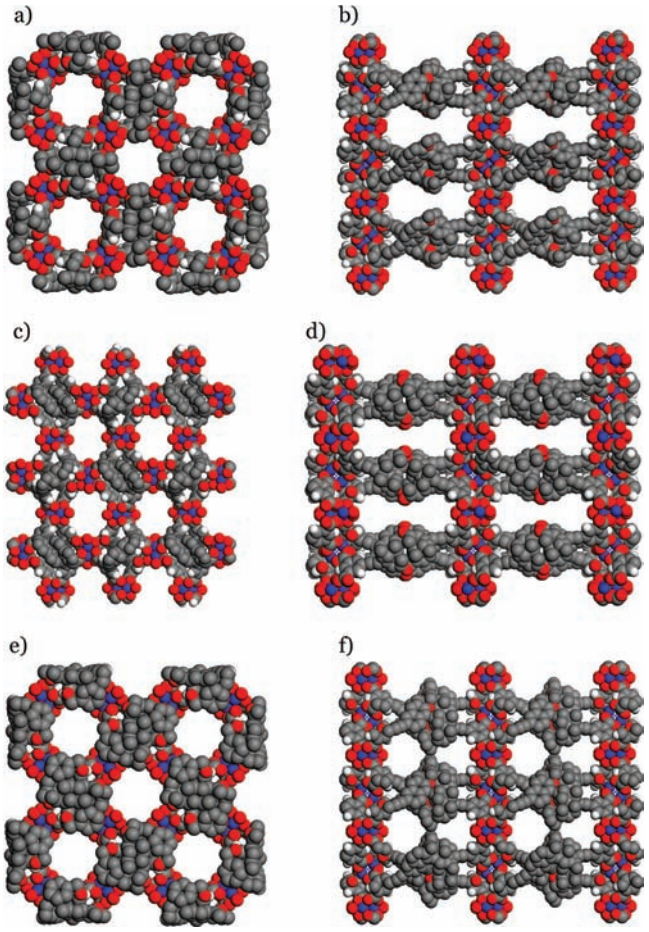

Figure 3. (a) Space-filling model of **1** as viewed down the *c* axis, showing open channels with the largest dimension of ~9.5 × 9.5 Å. (b) Space-filling model of **1** as viewed along the (110) direction, showing channels with the largest dimension of 16 Å. (c) Space-filling model of **2** as viewed down the *c* axis, showing open channels with dimensions of ~7 × 10.3 Å. (d) Space-filling model of **2** as viewed along the *b* axis, showing rectangular channels of ~9.2 × 16 Å. (e) Space-filling model of **3** as viewed down the *c* axis, showing open channels of ~7.2 × 7.2 Å. (f) Space-filling model of **3** as viewed along the (110) direction, showing two different open channels of ~6.0 × 6.7 and 6.7 × 7.8 Å.

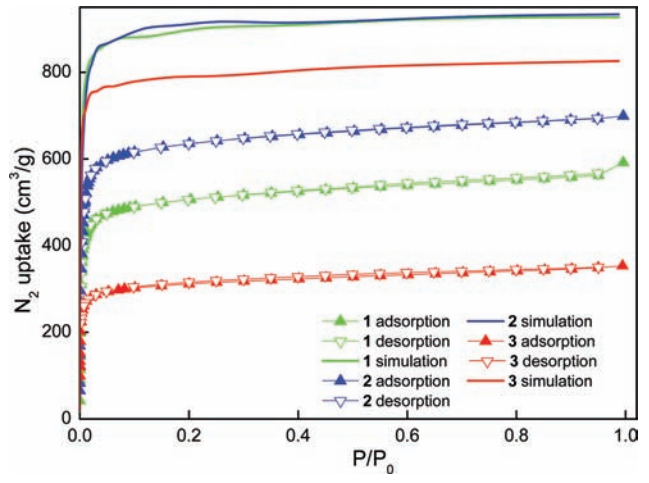

Figure 4. Experimental and calculated N_2 adsorption isotherms for **1**–**3**.

Table 1. Experimental and Calculated Surface Areas and Pore Volumes for 1–3[a]

	Langmuir surface area (m^2/g)	BET surface area (m^2/g)	pore volume (cc/g)	pore width (Å)
1	2245(3947)	1942(3526)	0.77(1.38)	5.52(7.22)
2	2819(4027)	2448(3565)	0.97(1.40)	5.37(7.62)
3	1323(3450)	1189(3094)	0.47(1.22)	5.82(6.67)

[a]Numbers in parentheses are calculated values.

calculated surface areas tend to be larger than the experimental results.

An HK cumulative pore size comparison shows that, on average, **2** has slightly larger pores that **1** while the pores in **3** are almost the same size as **1** but with smaller pore volume (Figure 5). This porosity trend is consistent with the increasing

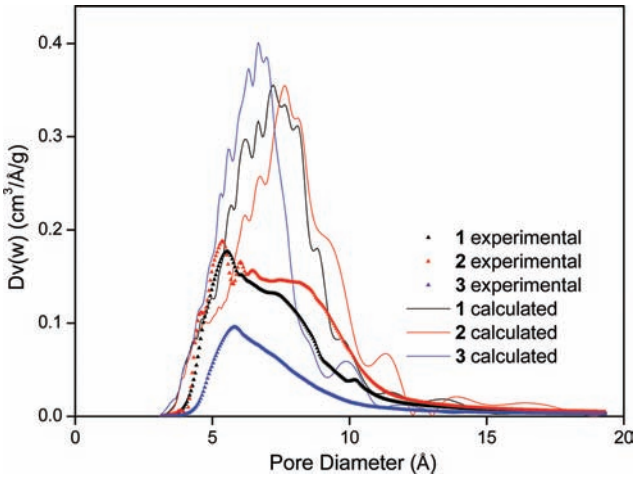

Figure 5. Experimental and calculated pore size distributions (HK method) for **1**–**3**.

steric bulk of hydroxy, ethoxy, and benzyloxy groups on the 2,2′-position of the binaphthyl moieties of the octacarboxylic acid bridging ligands. The HK cumulative pore volumes for **1**, **2**, and **3** were 0.77, 0.96, and 0.47 cm^3/g, respectively (Table 1). Theoretical simulations of pore distributions gave larger pore sizes and pore volumes than the experimental values (Figure 5).

3. Powder X-ray Diffraction Studies. Despite the different space groups, powder X-ray diffraction (PXRD) patterns of **1**, **2**, and **3** are very similar to each other, consistent with their isoreticular nature (Figure 6). However, when compared to the pristine samples, many of the PXRD peaks of the evacuated samples of **1**–**3** have disappeared, suggesting significant distortion of the framework structures (Figures 6 and S6 and S7, Supporting Information). The PXRD results are consistent with the gas adsorption experiments, where the experimental surface areas are significantly lower than the theoretical values.

Our earlier work indicates a high connectivity ligand can help in stabilizing the framework against distortion upon solvent removal.[69] Such a framework stabilization is also observed in the present MOF series as the related 4,4-connected MOFs built from shorter tetracarboxylic acid bridging ligands underwent severe framework distortion upon removal of the solvent molecules, leading to negligible surface areas as probed by gas adsorption measurements. However, the current study

dx.doi.org/10.1021/ic2024296 | *Inorg. Chem.* 2012, 51, 2503–2508

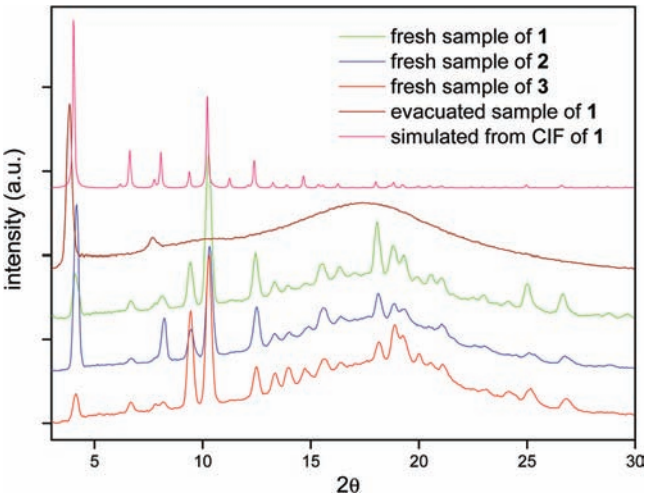

Figure 6. Powder X-ray diffraction patterns of fresh crystals of **1** (green), **2** (blue), and **3** (red) along with the evacuated sample of **1** (brown) and calculated PXRD pattern of **1** (pink).

also shows that the high network connectivity cannot completely prevent the framework distortion when the bridging ligands become much longer. Framework distortion can reduce the pore sizes of highly porous MOFs, leading to minimization of the framework energy. In this present MOF series, the carbon−carbon triple bond is slightly flexible to allow partial distortion without destroying the MOF structures.

4. Hydrogen Adsorption Studies. Hydrogen adsorption experiments show **1** uptakes 1.7 wt % hydrogen at 77 K and 1 atm. **2** has a hydrogen uptake of 1.8 wt %, while **3** is capable of adsorbing 1.4% hydrogen at 1 atm and 77 K (Figure 7). All of

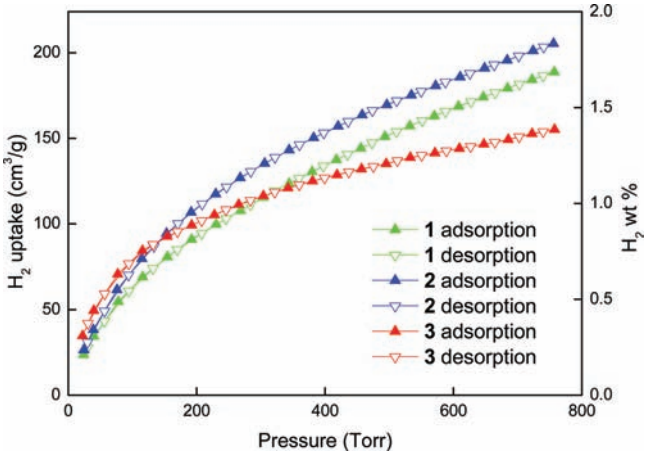

Figure 7. H_2 adsorption isotherms for **1**−**3**.

the present MOF series thus exhibit significant hydrogen storage capacities. However, hydrogen uptakes of MOFs **1**−**3** are lower than those of the similar MOFs built from the shorter 1,1′-binaphthyl-derived octacarboxylic acids (1.8−2.5 wt %), presumably as a result of framework distortion caused by the elongated bridging ligands.[69] The hydrogen uptake capacity of MOFs **1**−**3** correlates well with their surface areas. Bulkier substituent groups at the 2,2′-positions of the binaphthyl moieties lead to lower surface areas and lower hydrogen uptake capacity. This illustrates the ability to tune the surface area, pore size, and gas uptake by systematically changing the alkoxy groups of the octacarboxylic acid bridging ligands in **1**−**3**.

CONCLUSIONS

We synthesized highly porous and robust 4,8-connected MOFs based on rigid, aromatic-rich octacarboxylate ligands and copper paddle-wheel SBUs. The high network connectivity significantly stabilizes the framework of these MOFs, but some framework distortion still occurs as a result of the elongated bridging ligands. These MOFs exhibit large surface areas and significant hydrogen uptake. Our work thus reinforces the notion of designing highly porous, tunable, and functional MOFs using bridging ligands of high connectivity.

ASSOCIATED CONTENT

Supporting Information

Procedures for ligand synthesis and characterization, X-ray crystallographic data, Langmuir and BET plots, and powder X-ray diffraction patterns. This material is available free of charge via the Internet at http://pubs.acs.org.

AUTHOR INFORMATION

Corresponding Author

*Phone: 919-962-6320. Fax: 919-962-2388. E-mail: wlin@unc.edu.

Author Contributions

†These authors contributed equally to this work.

ACKNOWLEDGMENTS

We acknowledge financial support from the NSF (DMR-0906662).

REFERENCES

(1) Schlapbach, L.; Zuttel, A. *Nature* **2001**, *414*, 353.
(2) van den Berg, A. W. C.; Arean, C. O. *Chem. Commun.* **2008**, 668.
(3) Eberle, U.; Felderhoff, M.; Schuth, F. *Angew. Chem., Int. Ed.* **2009**, *48*, 6608.
(4) Orimo, S.-i.; Nakamori, Y.; Eliseo, J. R.; Zuettel, A.; Jensen, C. M. *Chem. Rev.* **2007**, *107*, 4111.
(5) Grochala, W.; Edwards, P. P. *Chem. Rev.* **2004**, *104*, 1283.
(6) Thomas, K. M. *Catal. Today* **2007**, *120*, 389.
(7) Ockwig, N. W.; Delgado-Friedrichs, O.; O'Keeffe, M.; Yaghi, O. M. *Acc. Chem. Res.* **2005**, *38*, 176.
(8) Kitagawa, S.; Kitaura, R.; Noro, S.-i. *Angew. Chem., Int. Ed.* **2004**, *43*, 2334.
(9) Férey, G.; Mellot-Draznieks, C.; Serre, C.; Millange, F. *Acc. Chem. Res.* **2005**, *38*, 217.
(10) Evans, O. R.; Lin, W. *Acc. Chem. Res.* **2002**, *35*, 511.
(11) Bradshaw, D.; Warren, J. E.; Rosseinsky, M. J. *Science* **2007**, *315*, 977.
(12) Sculley, J.; Yuan, D.; Zhou, H.-C. *Energy Environ. Sci.* **2011**, *4*, 2721.
(13) Rowsell, J. L. C.; Yaghi, O. M. *Angew. Chem., Int. Ed.* **2005**, *44*, 4670.
(14) Murray, L. J.; Dinca, M.; Long, J. R. *Chem. Soc. Rev.* **2009**, *38*, 1294.
(15) Chen, B.; Liang, C.; Yang, J.; Contreras, D. S.; Clancy, Y. L.; Lobkovsky, E. B.; Yaghi, O. M.; Dai, S. *Angew. Chem., Int. Ed.* **2006**, *45*, 1390.
(16) Yuan, G.; Zhu, C.; Xuan, W.; Cui, Y. *Chem.—Eur. J.* **2009**, *15*, 6428.
(17) Lee, C. Y.; Bae, Y. S.; Jeong, N. C.; Farha, O. K.; Sarjeant, A. A.; Stern, C. L.; Nickias, P.; Snurr, R. Q.; Hupp, J. T.; Nguyen, S. T. *J. Am. Chem. Soc.* **2011**, *133*, 5228.

(18) Xie, Z.; Ma, L.; deKrafft, K. E.; Jin, A.; Lin, W. *J. Am. Chem. Soc.* **2009**, *132*, 922.
(19) Lan, A.; Li, K.; Wu, H.; Olson, D. H.; Emge, T. J.; Ki, W.; Hong, M.; Li, J. *Angew. Chem., Int. Ed.* **2009**, *48*, 2334.
(20) Chen, B.; Wang, L.; Xiao, Y.; Fronczek, F. R.; Xue, M.; Cui, Y.; Qian, G. *Angew. Chem., Int. Ed.* **2009**, *48*, 500.
(21) Allendorf, M. D.; Houk, R. J. T.; Andruszkiewicz, L.; Talin, A. A.; Pikarsky, J.; Choudhury, A.; Gall, K. A.; Hesketh, P. J. *J. Am. Chem. Soc.* **2008**, *130*, 14404.
(22) Ma, L.; Abney, C.; Lin, W. *Chem. Soc. Rev.* **2009**, *38*, 1248.
(23) Lee, J.; Farha, O. K.; Roberts, J.; Scheidt, K. A.; Nguyen, S. T.; Hupp, J. T. *Chem. Soc. Rev.* **2009**, *38*, 1450.
(24) Kesanli, B.; Lin, W. *Coord. Chem. Rev.* **2003**, *246*, 305.
(25) Rieter, W. J.; Taylor, K. M. L.; An, H.; Lin, W.; Lin, W. *J. Am. Chem. Soc.* **2006**, *128*, 9024.
(26) deKrafft, K. E.; Xie, Z.; Cao, G.; Tran, S.; Ma, L.; Zhou, O. Z.; Lin, W. *Angew. Chem., Int. Ed.* **2009**, *48*, 9901.
(27) Liu, D.; Huxford, R. C.; Lin, W. *Angew. Chem., Int. Ed.* **2011**, *50*, 3696.
(28) Rieter, W. J.; Pott, K. M.; Taylor, K. M. L.; Lin, W. *J. Am. Chem. Soc.* **2008**, *130*, 11584.
(29) Horcajada, P.; Chalati, T.; Serre, C.; Gillet, B.; Sebrie, C.; Baati, T.; Eubank, J. F.; Heurtaux, D.; Clayette, P.; Kreuz, C.; Chang, J.-S.; Hwang, Y. K.; Marsaud, V.; Bories, P.-N.; Cynober, L.; Gil, S.; Férey, G.; Couvreur, P.; Gref, R. *Nat. Mater.* **2010**, *9*, 172.
(30) Taylor-Pashow, K. M. L.; Della Rocca, J.; Xie, Z.; Tran, S.; Lin, W. *J. Am. Chem. Soc.* **2009**, *131*, 14261.
(31) Rosi, N. L.; Eckert, J.; Eddaoudi, M.; Vodak, D. T.; Kim, J.; O'Keeffe, M.; Yaghi, O. M. *Science* **2003**, *300*, 1127.
(32) Dinca, M.; Dailly, A.; Liu, Y.; Brown, C. M.; Neumann, D. A.; Long, J. R. *J. Am. Chem. Soc.* **2006**, *128*, 16876.
(33) Latroche, M.; Surble, S.; Serre, C.; Mellot-Draznieks, C.; Llewellyn, P. L.; Lee, J.-H.; Chang, J.-S.; Jhung, S. H.; Ferey, G. *Angew. Chem., Int. Ed.* **2006**, *45*, 8227.
(34) Panella, B.; Hirscher, M.; Putter, H.; Muller, U. *Adv. Funct. Mater.* **2006**, *16*, 520.
(35) Rowsell, J. L. C.; Yaghi, O. M. *J. Am. Chem. Soc.* **2006**, *128*, 1304.
(36) Kaye, S. S.; Dailly, A.; Yaghi, O. M.; Long, J. R. *J. Am. Chem. Soc.* **2007**, *129*, 14176.
(37) Wang, X.-S.; Ma, S.; Forster, P. M.; Yuan, D.; Eckert, J.; Lopez, J. J.; Murphy, B. J.; Parise, J. B.; Zhou, H.-C. *Angew. Chem., Int. Ed.* **2008**, *47*, 7263.
(38) Cheon, Y. E.; Suh, M. P. *Chem. Commun.* **2009**, 2296.
(39) Lin, X.; Telepeni, I.; Blake, A. J.; Dailly, A.; Brown, C. M.; Simmons, J. M.; Zoppi, M.; Walker, G. S.; Thomas, K. M.; Mays, T. J.; Hubberstey, P.; Champness, N. R.; Schröder, M. *J. Am. Chem. Soc.* **2009**, *131*, 2159.
(40) Farha, O. K.; Yazaydin, A. O.; Eryazici, I.; Malliakas, C. D.; Hauser, B. G.; Kanatzidis, M. G.; Nguyen, S. T.; Snurr, R. Q.; Hupp, J. T. *Nat. Chem.* **2010**, *2*, 944.
(41) Furukawa, H.; Ko, N.; Go, Y. B.; Aratani, N.; Choi, S. B.; Choi, E.; Yazaydin, A. O.; Snurr, R. Q.; O'Keeffe, M.; Kim, J.; Yaghi, O. M. *Science* **2010**, *329*, 424.
(42) Ma, S.; Zhou, H.-C. *Chem. Commun.* **2010**, *46*, 44.
(43) Kesanli, B.; Cui, Y.; Smith, M. R.; Bittner, E. W.; Bockrath, B. C.; Lin, W. *Angew. Chem., Int. Ed. Engl.* **2004**, *44*, 72.
(44) Dincă, M.; Long, J. R. *Angew. Chem., Int. Ed.* **2008**, *47*, 6766.
(45) Eddaoudi, M.; Kim, J.; Rosi, N.; Vodak, D.; Wachter, J.; O'Keeffe, M.; Yaghi, O. M. *Science* **2002**, *295*, 469.
(46) Cavka, J. H.; Jakobsen, S.; Olsbye, U.; Guillou, N.; Lamberti, C.; Bordiga, S.; Lillerud, K. P. *J. Am. Chem. Soc.* **2008**, *130*, 13850.
(47) Zhang, J.-P.; Chen, X.-M. *Chem. Commun.* **2006**, 1689.
(48) Surble, S.; Serre, C.; Mellot-Draznieks, C.; Millange, F.; Férey, G. *Chem. Commun.* **2006**, 284.
(49) Chui, S. S.-Y.; Lo, S. M.-F.; Charmant, J. P. H; Orpen, A. G.; Williams, I. D. *Science* **1999**, *283*, 1148.
(50) Lee, J. Y.; Olson, D. H.; Pan, L.; Emge, T. J.; Li, J. *Adv. Funct. Mater.* **2007**, *17*, 1255.
(51) Chen, B.; Ma, S.; Zapata, F.; Fronczek, F. R.; Lobkovsky, E. B.; Zhou, H.-C. *Inorg. Chem.* **2007**, *46*, 1233.
(52) Pan, L.; Sander, M. B.; Huang, X.; Li, J.; Smith, M.; Bittner, E.; Bockrath, B.; Johnson, J. K. *J. Am. Chem. Soc.* **2004**, *126*, 1308.
(53) Ma, L.; Lee, J. Y.; Li, J.; Lin, W. *Inorg. Chem.* **2008**, *47*, 3955.
(54) Yan, Y.; Telepeni, I.; Yang, S.; Lin, X.; Kockelmann, W.; Dailly, A.; Blake, A. J.; Lewis, W.; Walker, G. S.; Allan, D. R.; Barnett, S. A.; Champness, N. R.; Schröder, M. *J. Am. Chem. Soc.* **2010**, *132*, 4092.
(55) Chen, B.; Ockwig, N. W.; Millward, A. R.; Contreras, D. S.; Yaghi, O. M. *Angew. Chem., Int. Ed.* **2005**, *44*, 4745.
(56) Hu, Y.; Xiang, S.; Zhang, W.; Zhang, Z.; Wang, L.; Bai, J.; Chen, B. *Chem. Commun.* **2009**, 7551.
(57) Xiao, B.; Wheatley, P. S.; Zhao, X. B.; Fletcher, A. J.; Fox, S.; Rossi, A. G.; Megson, I. L.; Bordiga, S.; Regli, L.; Thomas, K. M.; Morris, R. E. *J. Am. Chem. Soc.* **2007**, *129*, 1203.
(58) Carson, C. G.; Hardcastle, K.; Schwartz, J.; Liu, X.; Hoffmann, C.; Gerhardt, R. A.; Tannenbaum, R. *Eur. J. Inorg. Chem.* **2009**, *2009*, 2338.
(59) Wu, S.; Ma, L.; Long, L.-S.; Zheng, L.-S.; Lin, W. *Inorg. Chem.* **2009**, *48*, 2436.
(60) Ma, L.; Lin, W. *J. Am. Chem. Soc.* **2008**, *130*, 13834.
(61) Liu, D.; Xie, Z.; Ma, L.; Lin, W. *Inorg. Chem.* **2010**, *49*, 9107.
(62) Lin, X.; Jia, J.; Zhao, X.; Thomas, K. M.; Blake, A. J.; Walker, G. S.; Champness, N. R.; Hubberstey, P.; Schröder, M. *Angew. Chem., Int. Ed.* **2006**, *45*, 7358.
(63) Yan, Y.; Yang, S. H.; Blake, A. J.; Lewis, W.; Poirier, E.; Barnett, S. A.; Champness, N. R.; Schroder, M. *Chem. Commun.* **2011**, *47*, 9995.
(64) Yang, S. H.; Lin, X.; Dailly, A.; Blake, A. J.; Hubberstey, P.; Champness, N. R.; Schröder, M. *Chem.—Eur. J.* **2009**, *15*, 4829.
(65) Yan, Y.; Lin, X.; Yang, S.; Blake, A. J.; Dailly, A.; Champness, N. R.; Hubberstey, P.; Schröder, M. *Chem. Commun.* **2009**, 1025.
(66) Ma, S. Q.; Simmons, J. M.; Sun, D. F.; Yuan, D. Q.; Zhou, H. C. *Inorg. Chem.* **2009**, *48*, 5263.
(67) Guo, Z.; Wu, H.; Srinivas, G.; Zhou, Y.; Xiang, S.; Chen, Z.; Yang, Y.; Zhou, W.; O'Keeffe, M.; Chen, B. *Angew. Chem., Int. Ed.* **2011**, *50*, 3178.
(68) Ma, L.; Falkowski, J. M.; Abney, C.; Lin, W. *Nat Chem* **2010**, *2*, 838.
(69) Ma, L.; Mihalcik, D. J.; Lin, W. *J. Am. Chem. Soc.* **2009**, *131*, 4610.
(70) Tan, C.; Yang, S.; Champness, N. R.; Lin, X.; Blake, A. J.; Lewis, W.; Schröder, M. *Chem. Commun.* **2011**, *47*, 4487.
(71) Spek, A. L. *J. Appl. Crystallogr.* **2003**, *36*, 7.
(72) Ma, L.; Jin, A.; Xie, Z.; Lin, W. *Angew. Chem., Int. Ed.* **2009**, *48*, 9905.
(73) Walton, K. S.; Snurr, R. Q. *J. Am. Chem. Soc.* **2007**, *129*, 8552.
(74) Serre, C.; Millange, F.; Thouvenot, C.; Noguès, M.; Marsolier, G.; Louër, D.; Férey, G. *J. Am. Chem. Soc.* **2002**, *124*, 13519.
(75) Llewellyn, P. L.; Maurin, G.; Devic, T.; Loera-Serna, S.; Rosenbach, N.; Serre, C.; Bourrelly, S.; Horcajada, P.; Filinchuk, Y.; Férey, G. r. *J. Am. Chem. Soc.* **2008**, *130*, 12808.